Proceedings of the 9th International Conference of Control Dynamic Systems, and Robotics (CDSR'22)
Niagara Falls, Canada – June 02-04, 2022
Paper No. 124
DOI: 10.11159/cdsr22.124

Battery Energy Maximization of a Solar Powered Unmanned Ground Vehicle in an Unknown Environment

Luke Strebe[1], Kooktae Lee[2]
[1]New Mexico Tech
801 Leroy Pl., Socorro, USA
Luke.Strebe@student.nmt.edu; Kooktae.Lee@nmt.edu
[2]New Mexico Tech
801 Leroy Pl., Socorro, USA

Abstract - Solar powered unmanned ground vehicles (SPUGV) can be used to monitor remote points of interest. Heuristic algorithms have been developed for path planning of SPUGVs in known solar environments, however not all environments have detailed solar mapping. A control algorithm to prioritize the battery life of a SPUGV in an unknown solar environment as it moves to specified points of interest was developed. The algorithm incorporates a switching cost function where one cost function prioritizes the goal position when the battery on the SPUGV is above a set threshold and the other prioritizes finding solar irradiance peaks to charge the battery. Local solar irradiance peaks are identified by a filtering approach from collected data in a local sample area. From simulations, the algorithm results in the SPUGV reaching the point of interest with a higher battery charge than a direct path to the point without any prior solar mapping.

***Keywords*:** Solar Power, Unmanned Ground Vehicle, Mobile Robot, Battery Charge, Energy Maximization

1. Introduction

Environmental monitoring is very important to help determine the ecological health of an area. For example, animal population, foliage health, local weather information, air pollution, and water quality are all important factors that can be monitored using unmanned ground vehicles (UGV). These missions require a long-term process and are best done remotely, as a result, any UGVs sent into the field to study the environment need to survive for long periods of time and travel far distances [1]. With Ray [2], solar harvesting was used in order to have the "cool robot" SPUGV travel 500 km across Antarctica to conduct and run scientific experiments. Areas such as Antarctica have consistently high sources of solar irradiance (SI) so path planning towards a goal was focused on rough terrain and obstacle avoidance. Others such as Plonski [3, 4] developed an algorithm to construct a solar map for a defined area using an SPUGV for future path planning in the constructed solar map. Kaplan [5] developed a time-optimized path planning algorithm for a SPUGV in a known solar environment so that the robot minimized travel time while also moving through high SI points on its way to the goal in order to increase the battery life of the SPUGV. All of the approaches require significant planning and mapping of an area in order for the SPUGV to navigate through it. Also as Plonski [3] discusses, the solar environment in an area is constantly changing as the sun moves, so any solar mapping data may be inaccurate by the time the robot begins path planning.

Despite the research for path planning in known solar environments, little has been done for path planning in unknown solar environments. Current path planning techniques need detailed solar environment information for the SPUGV to traverse an environment which is not always feasible or reasonable. Solar environments are constantly changing each day and throughout the year, therefore path planning in an unknown solar environment would make environmental monitoring missions using UGV's a more viable option. A cost function switching (CFS) algorithm was developed to maximize the battery life of a SPUGV as it travels to points of interest in an unknown solar environment. The CFS proposed eliminates the need for prior solar information of an area for SPUGV path planning in environmental monitoring missions.

2. Problem Definition

Suppose a SPUGV is placed into an environment with a variety of SI intensities with the task to reach multiple points of interest and then to return to the starting position with the maximum battery life achievable. Figure 1 demonstrates a

discretized global solar map with the SI values ranging from high in red, to low in dark blue where X_1, X_2, and X_3 are points of interest in sequential order.

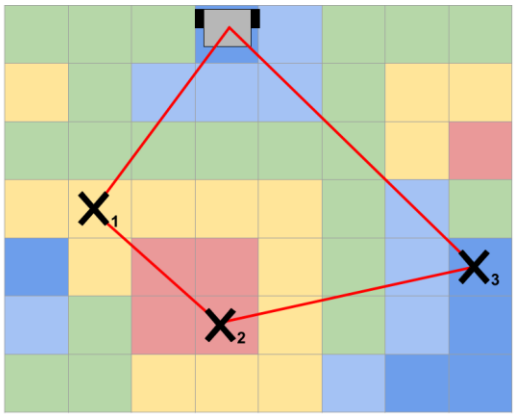

Fig. 1: Discretized basic solar map with multiple points of interest.

The problem can be defined as two path cost functions that seek to minimize the amount of energy expended when either moving towards a point of interest or a SI peak to charge. The first cost function J_1 seeks to minimize the control input cost with the goal position being the terminal cost. In equations (1) through (16), $x$is the SPUGV position, $x_g$is the goal position, $x_p$is the local energy peak position, and u is the control input. The constraints put upon both cost functions are that the control input is the velocity of the robot using basic dynamics, and that the input is limited to a set velocity max or $\underline{u_{max}}$. The initial and final states of the robot are defined as well. The J_2 cost function also minimizes the path cost of the input velocity, however the terminal cost is a sampled local SI peak instead of a point of interest or goal position.

$$\begin{aligned} \min J_1 = \int_t^{t+T} \frac{1}{2}||u||^2 dt + \phi_{fg} \\ \text{S.t. } x' = u \\ x(0) = x_0 \\ x(t_f) = x_f \\ \| u \| \leq u_{max} \end{aligned} \tag{1}$$

$$\begin{aligned} \min J_2 = \int_t^{t+T} \frac{1}{2}||u||^2 dt + \phi_{fp} \\ \text{S.t. } x' = u \\ x(0) = x_0 \\ x(t_f) = x_f \\ \| u \| \leq u_{max} \end{aligned} \tag{2}$$

The symbol ϕ_{fg} is the terminal cost of the goal and ϕ_{fp} is the terminal cost of the local SI peak.

$$\phi_{fg} = \frac{1}{2}||x(t) - x_g||^2 \tag{3}$$

$$\phi_{fp} = \frac{1}{2}||x(t) - x_p||^2 \tag{4}$$

With the cost functions defined, they can be optimized by two hamiltonian equations. The hamiltonian for J_1 is shown in equation (5), which looks identical to the hamiltonian for J_2.

$$H_1 = \frac{1}{2}||u||^2 + u \tag{5}$$

$$\frac{-\partial H_1}{\partial x} = \lambda' = \lambda_1^T = 0 \tag{6}$$

$$\frac{-\partial H_1}{\partial \lambda} = u = x' \tag{7}$$

$$\frac{-\partial H_1}{\partial u} = 0 = u^*(t) + \lambda \tag{8}$$

Equations (6) and (7) can be discretized and combined with equation (9) to find the optimized control input u^* in discrete time intervals.

$$\lambda(tf) = \frac{d\phi_{fg}}{dt_f} = x(t) - x_p \tag{9}$$

$$\lambda' = \frac{\lambda(t+1) - \lambda(t)}{\Delta t} = 0 \tag{10}$$

$$\lambda(t+)) = \lambda(t) \tag{11}$$

Likewise for equation (11), equation (7) can be rewritten into equation (12).

$$x(t+1) = (u^*(t) + x(t)) \cdot \Delta t \tag{12}$$

Because the costate variable $\lambda(t)$ is unchanging for both J_1 and J_1, therefore the problem is defined by four equations that provide the optimal path for J_1 and J_2 are shown in equations (13) through (16). Note that equation (13) is the costate variable definition for J_1 and equation (14) for J_2.

$$\lambda_{J2}[t] = x[t] - x_g \tag{13}$$

$$\lambda_{J1}[t] = x[t] - x_p \tag{14}$$

$$u^*[t] = -\lambda[t] \tag{15}$$

$$x^*[t+1] = x[t] + u^*[t] \tag{16}$$

At each time step, the optimization problems in (1) and (2) can be solved based on the Hamiltonian approach (5) - (16) in a receding-horizon manner [6 - 11]. This implies that after the local SI measurement using the onboard sensor, the SPUGV can determine where to go with a horizon length T, which is repeated at each time. This receding-horizon technique will enable the SPUGV to cope with a realistic scenario where a global SI map is not available and hence, the SPUGV needs to make a decision only with local information.

3. Main Result

3.1. Pathfinding Algorithm

In order to maximize the battery the robot needs to be able prioritize either charging the battery or reaching the goal at any given time, this was done by switching between solving for J_1 or J_2. We utilized a battery threshold as a switching criteria between the two functions. The battery threshold was set to 60% of the max battery so that the robot could travel long periods of time before recharging. Once the battery reaches 60% of the maximum battery life, the robot begins searching for nearby solar irradiance peaks. This is done with a sensing algorithm to determine the highest irradiance value with the closest distance to the goal. When a peak SI value is found, the robot will go towards the peak to charge the battery. The process of finding a SI peak is done continuously until the SPUGV reaches the local peak. The decision is made by observing four different variables, the SI at the current location, the SI at the measured peak, the distance from the current location to the peak, and the distance between the current location and the goal. If the robot has a lower measured SI than the peak and the distance to the peak is smaller than the distance to the goal, then the robot will move to the peak value as shown in Figure 2. If the robot has a SI larger than the measured peak, the robot is at a local maximum and will stay there until charged to a set upper charging threshold. If the goal distance is less than the distance to the peak, the robot will just go towards the goal. If none of these conditions are met, the robot will continue towards the goal to avoid getting stuck along the path.

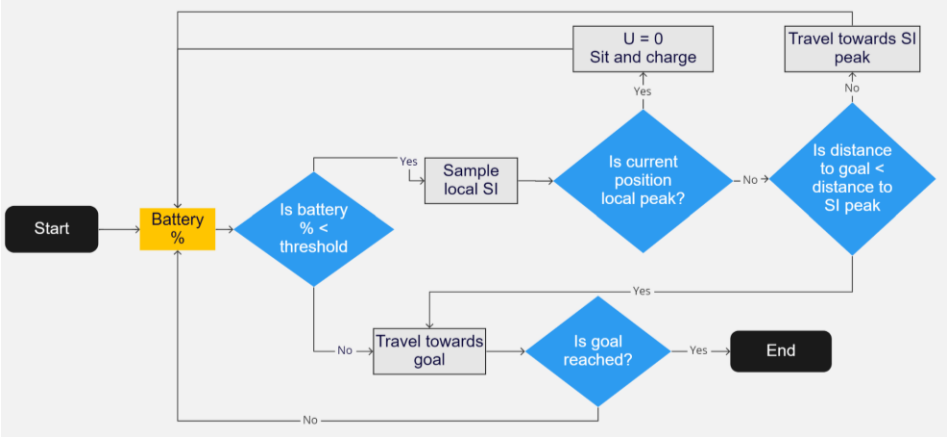

Fig. 2: Path planning algorithm flowchart.

3.2. Sensing Algorithm

Finding a single local SI peak requires another algorithm to detect and evaluate the SI around it. The sensing algorithm takes samples of a set sampling radius and step size and creates a sampling matrix of local SI values. An example sampling matrix is shown in Figure 3, the local sampled SI values also include the SI of the robots current position. Efficient evaluation of the samples was done by incorporating a statistical threshold so that only the highest SI values are observed. The threshold for peaks was set at 2 standard deviations from the mean of SI samples so that only the top 5% of SI in the local region are considered. The results from the thresholded sampling algorithm are multiple high SI peaks and their locations. Because the robot can only go towards one of the points, the sampling algorithm evaluates the SI at each local peak, the distance between the robot's current positions, and the distance between the peak and the goal position. By having distance as a method for determining the local max SI peak, the algorithm prioritizes energy peaks that are closer to the goal which prevents the robot from diverging away from the goal while searching for energy.

Figure 2 visualizes what the local sample from the robot looks like. The red squares indicate highest SI peaks while blue squares indicate lowest SI peaks. As shown in Figure 3, the SPUGV does not see the global solar information and can only see within the sample radius. With the thresholding, only two peaks would be considered for the local peak and therefore can be compared along with the distance directly to the goal from the robot to determine which path to be taken.

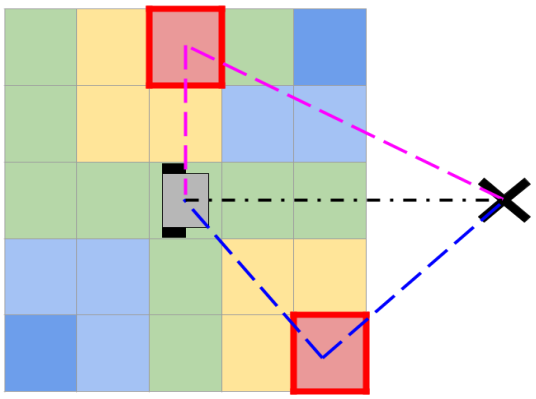

Fig. 3: Sensing algorithm example.

4. Simulations

4.1. Simulation Setup

In order to test the application of using the CFS algorithm, a solar environment was synthesized in the simulation. The environment was mapped in reference to a section of the Sante Fe National Forest in New Mexico, USA. The simulation uses multiple Gaussian distributions of SI that the robot can measure. New Mexico receives an average of 41.6 W/m^2 of SI

which is reflected in the solar map [12]. The high-intensity regions of the map indicate open areas such as a meadow in the forest with the assumption that the simulation is occurring when the sun is perpendicular to the ground and unchanging throughout the simulation. For simplicity, the simulation assumes that there are no inclination changes or obstacle obstructions that would be seen in the real environment. The robot chassis chosen for the simulation is the MLT-JR with two IG32 motors, two 2200maH batteries. The solar panel being simulated on the robot is an Eco-Worthy 10 W panel.

Fig. 4: MLT-JR, and Eco-Worthy 10W solar panel. .

The first simulation involved having the SPUGV travel from an initial position to a single point of interest, the SPUGV would start and end in a meadow where SI should be found. The distance between the two points was 2.5 km which is within the max distance the SPUGV can travel on one full charge of battery. The simulation was run using both the CFS algorithm and a direct route approach to determine if the battery at the goal position could be improved. The second simulation involved four points of interest on the same solar map as simulation 1. For simulation 2 SPUGV would start at an initial point and then travel to each point directly, only moving onto goal 3after arriving at goal 2 and so on. The total distance to travel to all the points sequentially was 2.5 km. The CSF algorithm was also compared to a direct route approach with multiple points of interest. Both simulations use a 5 m sensing radius for the SPUGV.

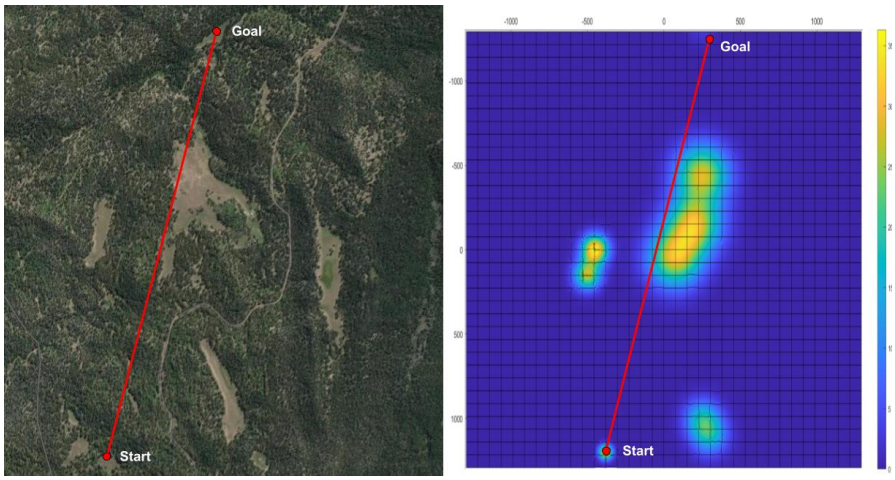

Fig. 5: Side by side of satellite image of map area and corresponding global solar map with a direct route trajectory.

4.2. Simulation Results

The simulation shown in table 1 and 2 demonstrates that the SPUGV using the CFS algorithm will reach the goal position with a significantly higher battery percentage than a direct route to the goal. For simulation 1 the trajectory of the SPUGV heads directly towards the goal until the battery threshold is met where it begins searching for SI peaks. Figure 4 shows the local peak SI values as bright green triangles. The path clearly shows the robot traveling towards the peak that is closest to the final goal. In the simulation the CFS algorithm took 166 minutes longer to reach the goal than the direct route, however, the CFS resulted in a 40.7% higher battery percentage at the goal. This shouldn't be a problem for applications like

environmental monitoring, where a sustainable operation of UGVs is much more important than the time taken. Likewise for the second simulation, the SPUGV took 333 minutes longer to complete the loop but with 70% more battery.

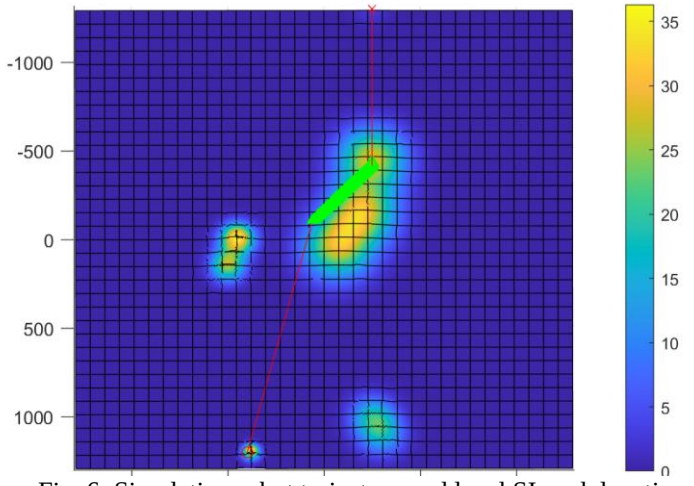

Fig. 6: Simulation robot trajectory and local SI peak locations.

Table 1: Simulation 1 battery and time results.

Algorithm	Time (minutes)	Battery % at t_f
None	49	24.2
CFS	215	64.9

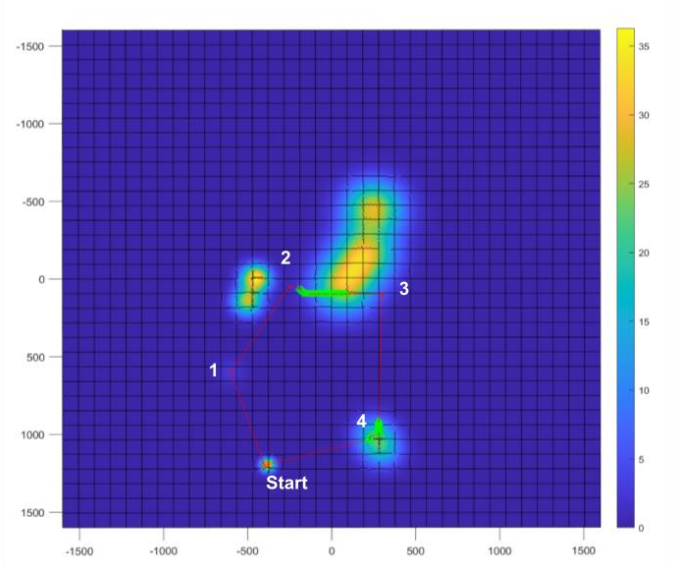

Fig. 7: Simulation robot trajectory and local SI peak locations.

Table 2: Simulation 2 battery and time results.

Algorithm	Time (minutes)	Battery % at t_f
None	69	0.7
CFS	402	71.0

5. Conclusion

Maximizing battery life during the mission such as environmental monitoring in an unknown environment is shown to be effectively done with a cost function switching algorithm. The proposed method, which prioritizes either the goal point or a local peak of SI depending on the remaining battery, guarantees that it will reach a point of interest with a higher battery life than going directly to a goal and therefore extend the mission life. As future works, we will further improve the proposed method including obstacle avoidance and SI peak masking to increase the effectiveness and robustness of the algorithm.

Acknowledgements

This research is partially supported by New Mexico Consortium Collaboration Grant with Dr. Steven J. Buelow as a prime contractor PI.

References

[1] J. Jones, G. Asner, S. Butchart, K. Karanth, "The 'why','what'and 'how'of monitoring for conservation." *Key topics in conservation biology 2*, pp. 327-343, 2013

[2] R. Laura, J, Lever, A. Street, A. Price, "Design and power management of a solar-powered "cool robot" for polar instrument networks." *Journal of Field Robotics* 24.7, pp. 581-599, 2007

[3] P. Plonski, J. Hook, and V. Isler, "Environment and solar map construction for solar-powered mobile systems." in *IEEE Transactions on Robotics* 32.1, pp. 70-82, 2016

[4] P. Plonski, P. Tokekar, and V. Isler, "Energy-efficient path planning for solar-powered mobile robots." *Journal of Field Robotics* 30.4, pp. 583-601, 2013

[5] A. Kaplan, N. Kingry, P. Uhing, R. Dai, "Time-optimal path planning with power schedules for a solar-powered ground robot." *IEEE Transactions on Automation Science and Engineering* 14.2, pp. 1235-1244, 2016

[6] K. Lee, S. Martínez, J. Cortés, R. H. Chen, and M. B. Milam, "Receding-horizon multi-objective optimization for disaster response," In *2018 Annual American Control Conference (ACC)*, pp. 5304-5309. IEEE, 2018.

[7] R. H. Kabir, and K. Lee, "On the ergodicity of an autonomous robot for efficient environment explorations," In *Dynamic Systems and Control Conference*, vol. 84287, p. V002T31A003. American Society of Mechanical Engineers, 2020.

[8] R. H. Kabir, and K. Lee, "Receding-horizon ergodic exploration planning using optimal transport theory," In *2020 American Control Conference (ACC)*, pp. 1447-1452. IEEE, 2020.

[9] R. H. Kabir, and K. Lee, "Wildlife monitoring using a multi-uav system with optimal transport theory," *Applied Sciences*, vol. 11, no. 9, p. 4070, 2021.

[10] R. H. Kabir, and K. Lee, "Efficient, decentralized, and collaborative multi-robot exploration using optimal transport theory," In *2021 American Control Conference (ACC)*, pp. 4203-4208. IEEE, 2021.

[11] K. Lee, and R. H. Kabir, "Density-aware decentralised multi-agent exploration with energy constraint based on optimal transport theory," *International Journal of Systems Science*, pp. 1-19, 2021.

[12] Direct Solar Irradiation (2020) [Online]. Available: http://www.ec.gc.ca/ges-ghg/default.asp?lang=En&n=040E378D-1